Synthesis of Heteronuclear Gold–Rhodium Cluster Compounds and Structural Characterisation of $[Rh(CNC_8H_9)_3(AuPPh_3)_5]^{2+}$, $[Rh(CNC_8H_9)_2(AuPPh_3)_6(AuCl)_2]^+$ and $[Rh(CO)_2(AuPPh_3)_7]^{2+}$ †

Simon G. Bott, Holm Fleischer, Mike Leach, D. Michael P. Mingos,* Harry Powell, David J. Watkin and Michael J. Watson

Inorganic Chemistry Laboratory, University of Oxford, South Parks Road, Oxford OX1 3QR, UK

The $NaBH_4$ reduction of a mixture of $[Au(PPh_3)Cl]$ and $[Rh(CNC_8H_9)_3Cl]$ leads to a dark red solution containing several Au–Rh cluster compounds, from which $[Rh(CNC_8H_9)_3(AuPPh_3)_5]^{2+}$ **1** and $[Rh(CNC_8H_9)_2(AuPPh_3)_6(AuCl)_2]^+$ **2** have been isolated. The cluster $[Rh(CO)_2(AuPPh_3)_7]^{2+}$ **3** has been synthesised by addition of 1 equivalent of $[Au(PPh_3)(NO_3)]$ to the tetrahydrofuran-soluble fraction of a solution obtained by the borohydride reduction of a mixture of $[Au(PPh_3)(NO_3)]$ and $[Rh(CO)_2(MeCN)_2]NO_3$. Compounds **1** and **3** have been characterised using ^{31}P-$\{^1H\}$ NMR, IR and fast atom bombardment mass spectroscopy and single-crystal X-ray techniques. Since **2** was formed only in low yield it has been characterised only by single-crystal X-ray diffraction methods. The structures of the three compounds are related and may be described as derivatives of a rhodium-centred Au_{12} icosahedron formed by removing four, five and seven vertices from the icosahedral cage.

Although a number of high-nuclearity gold cluster compounds with interstitial gold[1] or main-group atoms[2] have been characterised, only a few examples with incorporated transition metals are known. For example Bour *et al.*[3] have described the structure of $[Pt(AuPPh_3)_8]^{2+}$, which has a centred crown geometry analogous to that found in the isoelectronic cluster $[Au(AuPPh_3)_8]^{3+}$.[4] In addition, some other transition metal-centred gold cluster compounds with hemispherical topologies have been synthesised. Fig. 1 shows the idealised metal core geometries of $[Pt(PPh_3)(CO)(AuPPh_3)_5]^+$,[5] $[Pt(PPh_3)(CO)(AuPPh_3)_6]^{2+}$ (ref. 6) and $[Mo(CO)_3(AuPPh_3)_7]^+$ (ref. 7) as fragments of a centred icosahedron.

This paper describes the synthesis of some new gold–rhodium cluster compounds, with the rhodium atom occupying the interstitial site. As reported previously,[8] the $NaBH_4$ reduction of a mixture of monomeric gold and rhodium complexes provides an effective method for synthesising such compounds.

Results and Discussion

Addition of an ethanolic solution of $NaBH_4$ to an equimolar mixture of $[Au(PPh_3)Cl]$ and $[Rh(CNC_8H_9)_3Cl]$ suspended in ethanol yielded a dark red solution. Subsequent metathesis of this ethanolic solution with NH_4PF_6 led to a red precipitate which on recrystallisation from CH_2Cl_2–Et_2O gave yellow crystals of $[Rh(CNC_8H_9)_3(AuPPh_3)_5][PF_6]_2$ **1** in 27% yield. ^{31}P-$\{^1H\}$ NMR studies indicated that a number of gold–rhodium cluster compounds were present in the ethanolic solution after the removal of $[Rh(CNC_8H_9)_3(AuPPh_3)_5][PF_6]_2$. One of these compounds, $[Rh(CNC_8H_9)_2(AuPPh_3)_6(AuCl)_2]PF_6$ may be isolated in the form of red crystals suitable for a single-crystal X-ray diffraction study by layering the ethanolic solution with acetone and hexane. The complex $[Rh(CNC_8H_9)_3(AuPPh_3)_5][PF_6]_2$ has also been formed from the reaction of $[Au_8(PPh_3)_8]^{2+}$ with $[Rh(CNC_8H_9)_3Cl]$.

† *Supplementary data available:* see Instructions for Authors, *J. Chem. Soc., Dalton Trans.*, 1991, Issue 1, pp. xviii–xxii.

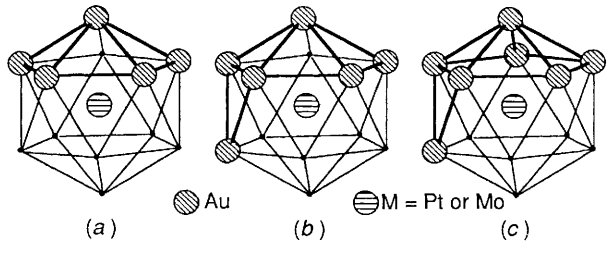

Fig. 1 Idealised metal core geometries of $[Pt(PPh_3)(CO)(AuPPh_3)_5]^+$ (*a*), $[Pt(PPh_3)(CO)(AuPPh_3)_6]^{2+}$ (*b*) and $[Mo(CO)_3(AuPPh_3)_7]^+$ (*c*) shown as fragments of a centred icosahedron

The infrared spectra of the PF_6^-, NO_3^- and ClO_4^- salts of complex **1** show the presence of terminal isocyanide ligands [ν(CN) at 2118 and 2085 cm^{-1}], phosphine ligands and the relevant unco-ordinated anions. The ^1H NMR spectrum exhibits a singlet in the methyl region at δ 1.92, indicating that all isocyanides are magnetically equivalent in solution. Integration of the spectrum gives a ratio of PPh_3 to isocyanide of 5:3. The ^{31}P-$\{^1H\}$ NMR spectrum of $[Rh(CNC_8H_9)_3(AuPPh_3)_5][PF_6]_2$ shows, in addition to the PF_6^- signal, a doublet with a coupling constant of 8.3 Hz at δ 37.1. The magnitude of this coupling constant is typical for the values measured for $^2J(Rh–P)$ coupling constants.

A positive-ion fast atom bombardment (FAB) mass spectrum of $[Rh(CNC_8H_9)_3(AuPPh_3)_5][PF_6]_2$ was recorded. An analysis of the isotopic ion-distribution pattern for the highest-mass peak gives a most-abundant mass ion at *m/z* 2937.38, which corresponds to the ion $[Rh(CNC_8H_9)_3(AuPPh_3)_5(PF_6)]^+$. A complete analysis of the fragmentation pattern suggests that the neutral compound is $[Rh(CNC_8H_9)_3(AuPPh_3)_5][PF_6]_2$. Confirmation of this assignment which is summarised in Table 1 has been achieved by recording the FAB mass spectrum of the nitrate salt, which results in a shift of peaks A, B and D. This information and the spectroscopic data described above allow the unambiguous formulation of the cluster compound **1** as $[Rh(CNC_8H_9)_3(AuPPh_3)_5][PF_6]_2$.

Information about the molecular geometry of the cluster ion

Table 1 Details of the positive-ion FAB mass spectrum of $[Rh(CNC_8H_9)_3(AuPPh_3)_5][PF_6]_2$; $M = [Rh(CNC_8H_9)_3(AuPPh_3)_5]$

Peak	m/z	Assignment	Relative abundance (%)
A	2937	$[M + PF_6]^+$	22
B	2806	$[M - CNC_8H_9 + PF_6]^+$	100
C	2661	$[M - CNC_8H_9]^+$	44
D	2544	$[M - CNC_8H_9 - PPh_3 + PF_6]$	13
E	2399	$[M - CNC_8H_9 - PPh_3]^+$	27
F	2333	$[M - Au - PPh_3]^+$	6
G	2201	$[M - Au - PPh_3 - CNC_8H_9]^+$	45

Table 2 Important bond lengths (Å) for compound **1**

Au(1)–Au(2)	2.830(2)	Au(1)–Au(3)	2.872(3)
Au(1)–Au(4)	2.985(2)	Au(1)–Rh	2.731(4)
Au(1)–P(1)	2.31(1)	Au(2)–Au(4)	2.865(2)
Au(2)–Au(5)	3.005(3)	Au(2)–Rh	2.683(5)
Au(2)–P(2)	2.31(1)	Au(3)–Au(4)	2.795(3)
Au(3)–Rh	2.681(3)	Au(3)–P(3)	2.27(1)
Au(4)–Au(5)	2.830(2)	Au(4)–Rh	2.720(4)
Au(4)–P(4)	2.30(1)	Au(5)–Rh	2.669(4)
Au(5)–P(5)	2.31(1)	Rh–C(1)	2.05(5)
Rh–C(2)	1.93(4)	Rh–C(3)	1.94(6)
N(1)–C(1)	1.13(4)	N(1)–C(11)	1.29(4)
N(2)–C(2)	1.14(4)	N(2)–C(21)	1.40(4)
N(3)–C(3)	1.18(5)	N(3)–C(31)	1.41(5)

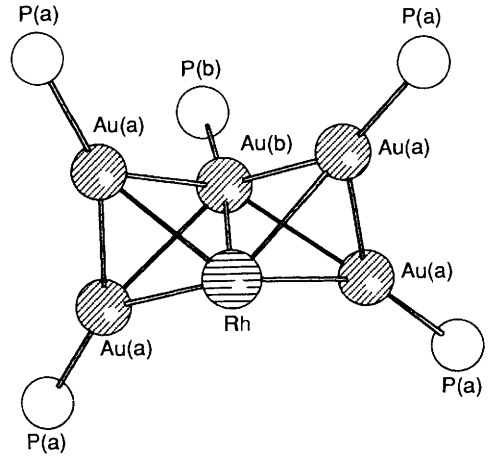

Fig. 2 Metal core geometry of $[Rh(CNC_8H_9)_3(AuPPh_3)_5]^{2+}$ **1** in solution showing the two distinct phosphorus environments

1 in solution was obtained from variable-temperature $^{31}P-\{^1H\}$ NMR spectra. The doublet observed in the spectrum at room temperature collapses to a sharp singlet at 260 K. Further cooling to 200 K gives a spectrum consisting of two broad resonances in a ratio of 4:1 but no $^3J(P-P)$ coupling is observed. This behaviour may be attributed to rapid intramolecular skeletal rearrangements which are a common feature in gold cluster chemistry.[9]

The low-temperture ^{31}P NMR spectrum is consistent with an edge-shared bitetrahedral metal cage geometry for **1** with the $Rh(CNC_8H_9)_3$ moiety at one of the most connected vertices (Fig. 2), analogous to the structure adopted by the isoelectronic compound $[ReH_4(PPh_3)_2(AuPPh_3)_5]^{2+}$.[10] Such a molecular geometry gives rise to four magnetically equivalent phosphine ligands (P_a) and a single inequivalent phosphine environment (P_b).

A single-crystal X-ray study on a suitable crystal of the ClO_4^- salt has demonstrated that **1** adopts a different molecular geometry in the solid state. Details of the analysis are given in the Experimental section, together with the relevant positional parameters. Selected intramolecular bond lengths and angles are summarised in Tables 2 and 3.

Table 3 Important bond angles (°) for compound **1**

Au(3)–Au(1)–Au(2)	105.20(7)	Au(4)–Au(1)–Au(2)	58.97(6)
Au(4)–Au(1)–Au(3)	56.97(6)	Rh–Au(1)–Au(2)	57.7(1)
Rh–Au(1)–Au(3)	57.11(9)	Rh–Au(1)–Au(4)	56.63(8)
Au(4)–Au(2)–Au(1)	63.21(6)	Au(5)–Au(2)–Au(1)	107.19(8)
Au(5)–Au(2)–Au(4)	57.57(6)	Rh–Au(2)–Au(1)	59.32(9)
Rh–Au(2)–Au(4)	58.61(8)	Rh–Au(2)–Au(5)	55.62(8)
Au(4)–Au(3)–Au(1)	63.56(7)	Rh–Au(3)–Au(1)	58.81(9)
Rh–Au(3)–Au(4)	59.53(9)	Au(2)–Au(4)–Au(1)	57.82(6)
Au(3)–Au(4)–Au(1)	59.47(6)	Au(3)–Au(4)–Au(2)	106.30(7)
Au(5)–Au(4)–Au(1)	107.75(7)	Au(5)–Au(4)–Au(2)	63.70(6)
Au(5)–Au(4)–Au(3)	105.44(8)	Rh–Au(4)–Au(1)	56.97(8)
Rh–Au(4)–Au(2)	57.3(1)	Rh–Au(4)–Au(3)	58.15(9)
Rh–Au(4)–Au(5)	57.45(8)	Au(4)–Au(5)–Au(2)	58.72(6)
Rh–Au(5)–Au(2)	56.1(1)	Rh–Au(5)–Au(4)	59.22(8)
Au(2)–Rh–Au(1)	63.0(1)	Au(3)–Rh–Au(1)	64.08(9)
Au(3)–Rh–Au(2)	115.2(1)	Au(4)–Rh–Au(1)	66.40(9)
Au(4)–Rh–Au(2)	64.0(1)	Au(4)–Rh–Au(3)	62.32(9)
Au(5)–Rh–Au(1)	120.9(1)	Au(5)–Rh–Au(2)	68.3(1)
Au(5)–Rh–Au(3)	113.5(1)	Au(5)–Rh–Au(4)	63.33(9)
C(3)–Rh–C(1)	98(2)	C(3)–Rh–C(2)	103(2)
C(11)–N(1)–C(1)	177(5)	C(21)–N(2)–C(2)	169(5)
C(31)–N(3)–C(3)	168(4)	N(1)–C(1)–Rh	165(4)
N(2)–C(2)–Rh	172(4)	N(3)–C(3)–Rh	170(4)

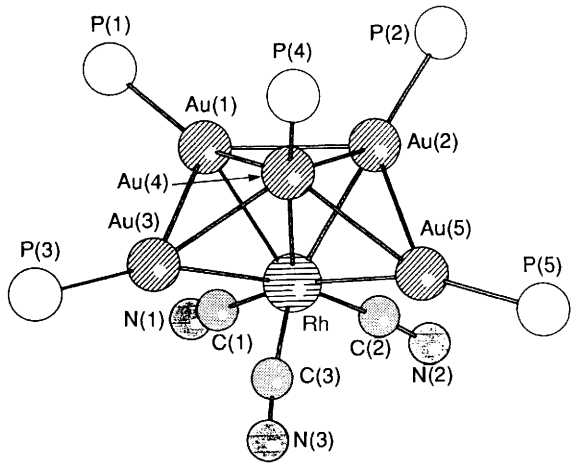

Fig. 3 Molecular structure of $[Rh(CNC_8H_9)_3(AuPPh_3)_5]^{2+}$ **1**. For reasons of clarity the phenyl and xylyl groups ave been omitted

The metal core in $[Rh(CNC_8H_9)_3(AuPPh_3)_5]^{2+}$ **1** may be described as bicapped tetrahedral with two $AuPPh_3$ groups capping two faces of a Au_3Rh tetrahedron with the $Rh(CNC_8H_9)_3$ moiety at the vertex common to both capped faces (Fig. 3). Alternatively, this skeletal geometry may be derived from a rhodium centred Au_{12} icosahedron by removal of a hemispherical bowl of seven Au atoms. The Au–Au distances in **1** fall in the range of 2.795(3)–3.005(3) Å and are comparable to those found in other high-nuclearity gold cluster compounds.[1] The Rh atom is bonded to five Au atoms with distances between 2.669(4) to 2.731(4) Å and to three almost linear isocyanide ligands [C–N–C 168(4)–177(5)°]. The existence of shorter radial than tangential bond distances is usual for metal-centred gold cluster compounds and underlines the greater importance of radial metal–metal bonding in these compounds.[11] This effect is anticipated to be further enhanced in transition metal-centred gold cluster compounds, as molecular orbital calculations have indicated that the transition metal occupies the central site in the cluster when Au–M bonds are stronger than Au–Au bonds.[12] The solid-state structure of $[Rh(CNC_8H_9)_3(AuPPh_3)_5]^{2+}$ **1** is analogous to that

Table 4 Important bond lengths (Å) for compound **2**

Au(1)–Au(2)	2.799(2)	Au(1)–Au(5)	2.869(2)
Au(1)–Au(8)	2.901(2)	Au(1)–Rh	2.708(3)
Au(1)–P(1)	2.27(1)	Au(2)–Au(6)	2.909(2)
Au(2)–Au(8)	2.793(2)	Au(2)–Rh	2.779(3)
Au(2)–P(2)	2.280(9)	Au(3)–Au(4)	2.800(2)
Au(3)–Au(6)	2.878(2)	Au(3)–Au(7)	2.891(2)
Au(3)–Rh	2.724(3)	Au(3)–P(3)	2.287(9)
Au(4)–Au(5)	2.822(2)	Au(4)–Au(7)	2.848(2)
Au(4)–Rh	2.771(3)	Au(4)–P(4)	2.28(1)
Au(5)–Au(7)	2.864(2)	Au(5)–Au(8)	2.785(2)
Au(5)–Rh	2.700(3)	Au(5)–Cl(1)	2.341(9)
Au(6)–Au(7)	2.781(2)	Au(6)–Au(8)	2.854(2)
Au(6)–Rh	2.654(3)	Au(6)–Cl(2)	2.310(9)
Au(7)–Au(8)	3.009(2)	Au(7)–Rh	2.819(3)
Au(7)–P(7)	2.278(9)	Au(8)–Rh	2.815(3)
Au(8)–P(8)	2.30(1)	Rh–C(109)	1.81(4)
Rh–C(118)	1.82(3)	N(1)–C(109)	1.25(4)
N(2)–C(118)	1.28(4)		

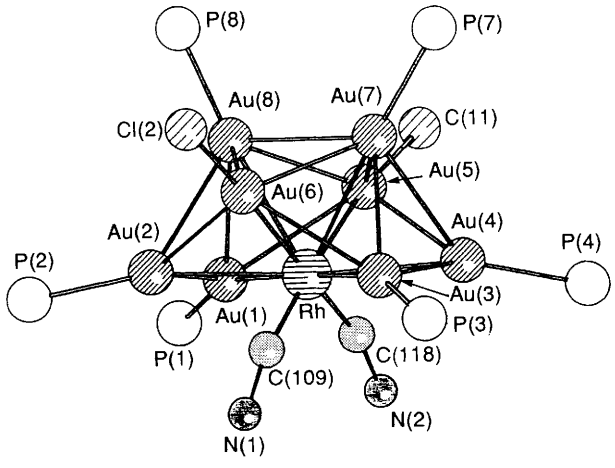

Fig. 4 Molecular structure of $[Rh(CNC_8H_9)_2(AuPPh_3)_6(AuCl)_2]^+$ **2**. For reasons of clarity the phenyl and xylyl groups have been omitted

established for the isoelectronic compound $[Pt(PPh_3)(CO)(AuPPh_3)_5]^+$.[5]

Extended-Hückel molecular orbital (EHMO) calculations on $[Rh(CNH)_3(AuPH_3)_5]^{2+}$ have indicated that the compound is only by 0.06 eV (9.6×10^{-21} *J*) more stable in the bicapped tetrahedral than in the edge-shared bitetrahedral geometry. This suggests that the variable-temperature ^{31}P-$\{^1H\}$ NMR spectra of **1** may be interpreted in terms of an intramolecular rearrangement between the two possible skeletal geometries based on the bicapped tetrahedron with the fused bitetrahedral geometry as an intermediate.

The ^{31}P-$\{^1H\}$ NMR spectrum of $[Rh(CNC_8H_9)_2(AuPPh_3)_6(AuCl)_2]PF_6$ **2** shows a doublet at δ 40.9 with a coupling constant $^2J(Rh–P) = 9.6$ Hz. Because of its low yield the compound was not amenable to a complete characterisation by standard spectroscopic methods and a single-crystal X-ray diffraction study was undertaken.[8] Details of the analysis are given in the Experimental section, together with the relevant positional parameters. Selected intramolecular bond distances and angles are given in Tables 4 and 5.

The skeletal geometry of compound **2** is shown in Fig. 4. Although no symmetry is crystallographically imposed, the metal cage has approximately C_{2v} symmetry. The gold atoms define a hemispherical bowl with the rhodium atom occupying a central position in the top face. Alternatively, the structure may be derived from a rhodium-centred icosahedron, with the eight gold atoms occupying the vertices, which remain after a butterfly of four atoms has been removed. The peripheral Au–Au bond lengths are similar to those in $[Rh(CNC_8H_9)_3(AuPPh_3)_5]^{2+}$ **1** and fall in the range 2.781(2)–3.009(2) Å. The rhodium atom has a particularly interesting and unusual co-ordination environment since it is bonded to eight Au atoms and to two terminal isocyanide ligands, which lie *trans* to the AuCl groups. The Rh–Au bond lengths to the less sterically crowded AuCl fragments [2.700(3) and 2.654(3) Å] are shorter than those to the remaining $AuPPh_3$ groups [2.708(3)–2.819(3) Å]. Similar observations have been made for the radial gold–gold distances found in the homonuclear gold cluster compounds $[Au_{10}Cl_3\{P(C_6H_{11})_2Ph\}_6]NO_3$ and $[Au_{13}Cl_2(PMe_2Ph)_{10}][PF_6]_3$.[13] The radial Au–Rh distances are considerably shorter than the peripheral Au–Au distances, a feature noted above for **1**. Since this structural characterisation[8] was undertaken, $[Pt(CO)(AuPPh_3)_8][NO_3]_2$ has been synthesised by the reaction of $[Pt(AuPPh_3)_8][NO_3]_2$ with carbon monoxide and shown to have a similar metal cage geometry.[14] Both clusters are characterised by 114 valence electrons and are isoelectronic with the gold cluster compound $[Au(AuPPh_3)_8]^+$. This homonuclear gold cluster has a centred cubic geometry however.[15]

A more rational precursor to the $Rh(CNC_8H_9)_2$ group found in **2** is the compound *trans*-$[Rh(CNC_8H_9)_2(CO)Cl]$. Although a ^{31}P-$\{^1H\}$ NMR study of the borohydride reduction of a 1:1 mixture of *trans*-$[Rh(CNC_8H_9)_2(CO)Cl]$ and $[Au(PPh_3)Cl]$ has demonstrated that **2** is formed in high yield, a satisfactory separation of the products could not be achieved. However this experiment suggests that cluster compounds with higher nuclearity are formed in better yields when rhodium precursors with more labile ligands are used.

The system $NaBH_4$–$[Au(PPh_3)(NO_3)]$–$[Rh(CO)_2(MeCN)_2]NO_3$ was investigated to explore the consequences of this suggestion. The complex $[Rh(CO)_2(MeCN)_2]NO_3$ was synthesised *in situ* by the reaction of $[Rh_2(\mu\text{-}Cl)_2(CO)_4]$ with $AgNO_3$ in acetonitrile. A dark red solution formed after the addition of a $NaBH_4$ solution in ethanol to the mixture of $[Rh(CO)_2(MeCN)_2]NO_3$ and $[Au(PPh_3)(NO_3)]$ in acetonitrile. Using a gold to rhodium ratio of 5:1 it has proved possible to isolate a tetrahydrofuran (thf) insoluble product. Addition of a solution of another equivalent of $[Au(PPh_3)(NO_3)]$ in thf to the remaining thf solution resulted in the formation of more of this insoluble product. This solid was readily recrystallised from CH_2Cl_2–Et_2O to give orange-red crystals, which have been characterised as $[Rh(CO)_2(AuPPh_3)_7][NO_3]_2$ **3** on the basis of spectroscopic data and a single-crystal X-ray diffraction study. The reaction of $[Rh_2(\mu\text{-}Cl)_2(CO)_4]$ with $[Au_8(PPh_3)_8][NO_3]_2$ provides an alternative synthetic route to this compound.

The IR spectrum of $[Rh(CO)_2(AuPPh_3)_7][NO_3]_2$ exhibits bands due to terminal carbonyl ligands [ν(CO) at 1965 and 1943 cm^{-1}] and unco-ordinated nitrate anions [$\nu(NO_3^-)$ at 1377 cm^{-1}]. The FAB mass spectrum has a highest-mass peak at *m/z* 3375, which corresponds to the ion $[Rh(CO)_2(AuPPh_3)_7]^+$. Characteristic fragmentation patterns due to the loss of phosphine and carbonyl ligands and gold atoms are also observed. The formulation of **3** as a dication is confirmed by the presence in the mass spectrum of a peak at *m/z* 3148, which has been assigned to the molecular ion $[M - CO - PPh_3 + NO_3]^+$. The ^{31}P-$\{^1H\}$ NMR spectrum shows a doublet at δ 41.85 with a splitting of 9.1 Hz, which is indicative of a $^2J(Rh–P)$ coupling constant.

In addition compound **3** was characterised by a single-crystal X-ray diffraction analysis. Details are given in the Experimental section, together with the relevant positional parameters. The molecular structure is illustrated in Fig. 5 and selected bond distances and angles are listed in Tables 6 and 7. The cluster consists of a central rhodium atom bonded to seven peripheral $AuPPh_3$ units and two terminally co-ordinated carbonyl ligands. The metal atoms define an Au_6Rh pentagonal bipyramid with the rhodium atom in an axial position and with an additional $AuPPh_3$ fragment bridging a Au_2Rh triangular face in μ_3 fashion. Alternatively, the metal cage may be

Table 5 Important bond angles (°) for compound **2**

Au(5)–Au(1)–Au(2)	106.16(6)	Au(8)–Au(1)–Au(2)	58.64(5)	Rh–Au(7)–Au(3)	56.97(7)	Rh–Au(7)–Au(4)	58.54(6)
Au(8)–Au(1)–Au(5)	57.72(4)	Rh–Au(1)–Au(2)	60.58(6)	Rh–Au(7)–Au(5)	56.71(6)	Rh–Au(7)–Au(6)	56.58(6)
Rh–Au(1)–Au(5)	57.81(7)	Rh–Au(1)–Au(8)	60.14(7)	Rh–Au(7)–Au(8)	57.65(7)	Au(2)–Au(8)–Au(1)	58.86(5)
Au(6)–Au(2)–Au(1)	106.37(6)	Au(8)–Au(2)–Au(1)	62.50(5)	Au(5)–Au(8)–Au(1)	60.57(5)	Au(5)–Au(8)–Au(2)	108.68(6)
Au(8)–Au(2)–Au(6)	60.03(5)	Rh–Au(2)–Au(1)	58.08(6)	Au(6)–Au(8)–Au(1)	105.15(6)	Au(6)–Au(8)–Au(2)	62.01(5)
Rh–Au(2)–Au(6)	55.58(6)	Rh–Au(2)–Au(8)	60.70(7)	Au(6)–Au(8)–Au(5)	103.71(6)	Au(7)–Au(8)–Au(1)	106.59(5)
Au(6)–Au(3)–Au(3)	104.45(6)	Au(7)–Au(3)–Au(4)	60.04(5)	Au(7)–Au(8)–Au(2)	108.53(5)	Au(7)–Au(8)–Au(5)	59.10(5)
Au(7)–Au(3)–Au(6)	56.54(4)	Rh–Au(3)–Au(4)	60.20(6)	Au(7)–Au(8)–Au(6)	56.55(5)	Rh–Au(8)–Au(1)	56.52(6)
Rh–Au(3)–Au(6)	55.27(6)	Rh–Au(3)–Au(7)	60.19(6)	Rh–Au(8)–Au(2)	59.41(6)	Rh–Au(8)–Au(5)	57.63(6)
Au(5)–Au(4)–Au(3)	108.26(6)	Au(7)–Au(4)–Au(3)	61.57(5)	Rh–Au(8)–Au(6)	55.83(6)	Rh–Au(8)–Au(7)	57.78(6)
Au(7)–Au(4)–Au(5)	56.54(4)	Rh–Au(4)–Au(3)	60.20(6)	Au(2)–Rh–Au(1)	61.34(7)	Au(3)–Rh–Au(1)	175.8(1)
Rh–Au(4)–Au(6)	55.27(6)	Rh–Au(4)–Au(7)	60.21(6)	Au(3)–Rh–Au(2)	122.5(1)	Au(4)–Rh–Au(1)	115.16(9)
Au(4)–Au(5)–Au(1)	108.69(6)	Au(7)–Au(5)–Au(1)	111.48(6)	Au(4)–Rh–Au(2)	173.4(1)	Au(4)–Rh–Au(3)	61.26(7)
Au(7)–Au(5)–Au(4)	60.10(5)	Au(8)–Au(5)–Au(1)	61.71(5)	Au(5)–Rh–Au(1)	64.10(7)	Au(5)–Rh–Au(2)	111.6(1)
Au(8)–Au(5)–Au(4)	113.01(6)	Au(8)–Au(5)–Au(7)	64.35(5)	Au(5)–Rh–Au(3)	114.3(1)	Au(5)–Rh–Au(4)	62.10(7)
Rh–Au(5)–Au(1)	58.09(7)	Rh–Au(5)–Au(4)	60.19(7)	Au(6)–Rh–Au(1)	116.9(1)	Au(6)–Rh–Au(2)	64.71(7)
Rh–Au(5)–Au(7)	58.09(7)	Rh–Au(5)–Au(8)	61.74(7)	Au(6)–Rh–Au(3)	67.24(8)	Au(6)–Rh–Au(4)	114.1(1)
Au(3)–Au(6)–Au(2)	110.02(6)	Au(7)–Au(6)–Au(2)	111.76(6)	Au(6)–Rh–Au(5)	111.9(1)	Au(7)–Rh–Au(1)	118.1(1)
Au(7)–Au(6)–Au(3)	60.14(5)	Au(8)–Au(6)–Au(2)	57.96(5)	Au(7)–Rh–Au(2)	114.6(1)	Au(7)–Rh–Au(3)	62.48(7)
Au(8)–Au(6)–Au(3)	110.40(5)	Au(8)–Au(6)–Au(7)	64.54(5)	Au(7)–Rh–Au(4)	61.25(7)	Au(7)–Rh–Au(5)	62.49(7)
Rh–Au(6)–Au(2)	59.72(7)	Rh–Au(6)–Au(3)	57.49(7)	Au(7)–Rh–Au(6)	60.99(7)	Au(8)–Rh–Au(1)	63.34(7)
Rh–Au(6)–Au(7)	62.43(7)	Rh–Au(6)–Au(8)	61.34(7)	Au(8)–Rh–Au(2)	59.90(7)	Au(8)–Rh–Au(3)	119.7(7)
Au(4)–Au(7)–Au(3)	58.39(5)	Au(5)–Au(7)–Au(3)	104.65(5)	Au(8)–Rh–Au(4)	113.7(1)	Au(8)–Rh–Au(5)	60.63(7)
Au(5)–Au(7)–Au(4)	59.21(5)	Au(6)–Au(7)–Au(3)	63.32(5)	Au(8)–Rh–Au(6)	62.83(7)	Au(8)–Rh–Au(7)	64.57(7)
Au(6)–Au(7)–Au(4)	108.49(6)	Au(6)–Au(7)–Au(5)	103.56(6)	C(118)–Rh–C(109)	97(2)	C(110)–N(1)–C(109)	165(3)
Au(8)–Au(7)–Au(3)	108.54(5)	Au(8)–Au(7)–Au(4)	105.91(5)	C(119)–N(2)–C(118)	166(3)	N(1)–C(109)–Rh	163(3)
Au(8)–Au(7)–Au(5)	56.55(4)	Au(8)–Au(7)–Au(6)	58.91(5)	N(2)–C(118)–Rh	164(3)		

Table 6 Important bond lengths (Å) for compound **3**

Au(1)–Au(2)	3.102(5)	Au(1)–Au(3)	2.891(6)
Au(1)–Au(4)	2.856(4)	Au(1)–Au(5)	3.118(5)
Au(1)–Au(6)	2.788(4)	Au(1)–Rh	2.712(6)
Au(1)–P(1)	2.31(2)	Au(2)–Au(3)	2.894(4)
Au(2)–Au(6)	3.051(7)	Au(2)–Au(7)	2.892(5)
Au(2)–Rh	2.703(7)	Au(2)–P(2)	2.30(2)
Au(3)–Au(4)	2.899(6)	Au(3)–Au(7)	2.831(4)
Au(3)–Rh	2.765(8)	Au(3)–P(3)	2.32(2)
Au(4)–Au(5)	2.884(5)	Au(4)–Rh	2.734(6)
Au(4)–P(4)	2.31(2)	Au(5)–Au(6)	2.916(4)
Au(5)–Rh	2.64(1)	Au(5)–P(5)	2.33(3)
Au(6)–Rh	2.749(7)	Au(6)–P(6)	2.28(2)
Au(7)–Rh	2.72(1)	Au(7)–P(7)	2.27(3)
Rh–C(1)	1.96(4)	Rh–C(2)	1.94(5)
O(1)–C(1)	1.02(4)	O(2)–C(2)	1.04(4)

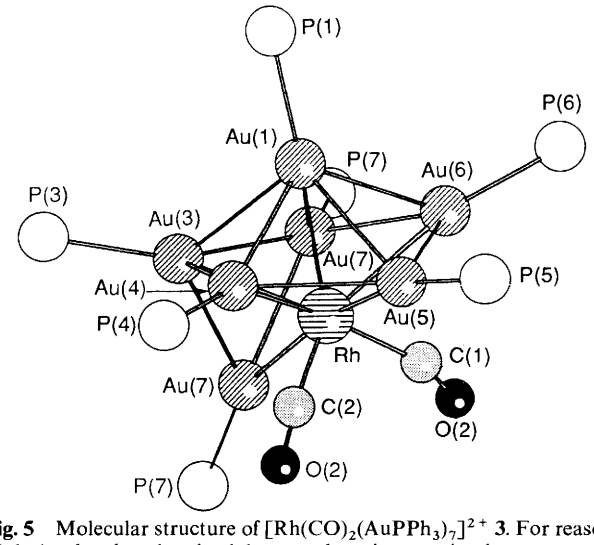

Fig. 5 Molecular structure of $[Rh(CO)_2(AuPPh_3)_7]^{2+}$ **3**. For reasons of clarity the phenyl and xylyl groups have been omitted

described as a fragment of a rhodium-centred icosahedron. The seven $AuPPh_3$ groups occupy the positions that remain after removal of five vertices from the icosahedron. The Au–Rh bond lengths fall in the range 2.64(1)–2.765(8) Å and are slightly shorter than the Au–Rh distances found in **1** and **2**. The peripheral Au–Au bonds vary in length from 2.788(4) to 3.118(5) Å and are slightly longer than in both cluster compounds discussed previously. The carbonyl ligands bonded to the rhodium form an angle of 95(2)° to one another and are slightly bent [Rh–C–O 159(9) and 161(8)°], presumably for steric reasons. The skeletal geometry of $[Rh(CO)_2(AuPPh_3)_7]^{2+}$ **3** is also adopted in the isoelectronic cluster compounds $[Mo(CO)_3(AuPPh_3)_7]^+$ (ref. 7) and $[Pt(PPh_3)(HgNO_3)_2(AuPPh_3)_5]^+$.[16]

The ^{31}P-$\{^1H\}$ NMR spectrum of the thf-soluble fraction of the reaction described above exhibits mainly a doublet at δ 41.03 with a ^2J(Rh–P) coupling constant of 11.5 Hz, due to the precursor, which reacts with 1 equivalent of $[Au(PPh_3)(NO_3)]$ to give $[Rh(CO)_2(AuPPh_3)_7]^{2+}$ **3**. The IR spectrum of the same fraction indicates the presence of terminal carbonyl ligands [ν(CO) 1944 and 1913 cm^{-1}] and unco-ordinated NO_3^- [$\nu(NO_3^-)$ 1378 cm^{-1}]. To date we have not been able to characterise this compound by FAB mass spectrometry or single-crystal methods.

According to ^{31}P-$\{^1H\}$ NMR investigations the same compound is formed by the reaction of $[Rh(CO)_2(AuPPh_3)_7]$-$[NO_3]_2$ with an excess of PPh_3. The results suggest the existence of equilibrium (1), which is analogous to that

$$[Rh(CO)_2(AuPPh_3)_7]^{2+} + PPh_3 \rightleftharpoons \underset{\mathbf{3}}{} [Rh(CO)_2(AuPPh_3)_6]^+ + [Au(PPh_3)_2]^+ \quad (1)$$
$$\mathbf{4}$$

established for the conversion of $[Au_9(PPh_3)_8]^{3+}$ into $[Au_8(PPh_3)_8]^{2+}$ by addition of an excess of PPh_3.[17] This suggests the tentative formulation of the intermediate, which leads to the formation of $[Rh(CO)_2(AuPPh_3)_7][NO_3]_2$ after addition of 1 equivalent of $[Au(PPh_3)(NO_3)]$, as $[Rh(CO)_2(AuPPh_3)_6]NO_3$.

The compound $[Rh(CO)_2(AuPPh_3)_6]^+$ **4** has a total of 90 valence electrons and is isoelectronic with $[Pt(PPh_3)(CO)$-

Table 7 Important angles (°) for compound **3**

Au(3)–Au(1)–Au(2)	57.6(1)	Au(4)–Au(1)–Au(2)	104.7(1)	Au(6)–Au(5)–Au(1)	54.9(1)	Au(6)–Au(5)–Au(4)	104.9(2)
Au(4)–Au(1)–Au(3)	60.6(1)	Au(5)–Au(1)–Au(2)	101.9(1)	Rh–Au(5)–Au(1)	55.5(2)	Rh–Au(5)–Au(4)	59.2(2)
Au(5)–Au(1)–Au(3)	103.9(1)	Au(5)–Au(1)–Au(4)	57.5(1)	Rh–Au(5)–Au(6)	59.1(2)	P(5)–Au(5)–Au(1)	137.5(5)
Au(6)–Au(1)–Au(2)	62.1(1)	Au(6)–Au(1)–Au(3)	110.7(2)	P(5)–Au(5)–Au(4)	129.1(5)	P(5)–Au(5)–Au(6)	121.1(5)
Au(6)–Au(1)–Au(4)	109.1(1)	Au(6)–Au(1)–Au(5)	58.9(1)	P(5)–Au(5)–Rh	166.1(5)	Au(2)–Au(6)–Au(1)	64.0(1)
Rh–Au(1)–Au(2)	54.9(2)	Rh–Au(1)–Au(3)	59.0(2)	Au(5)–Au(6)–Au(1)	66.2(1)	Au(5)–Au(6)–Au(2)	108.0(2)
Rh–Au(1)–Au(4)	58.7(1)	Rh–Au(1)–Au(5)	53.2(2)	Rh–Au(6)–Au(1)	58.7(1)	Rh–Au(6)–Au(2)	55.3(2)
Rh–Au(1)–Au(6)	59.9(2)	P(1)–Au(1)–Au(2)	117.4(5)	Rh–Au(6)–Au(5)	55.4(2)	P(6)–Au(6)–Au(1)	133.6(5)
P(1)–Au(1)–Au(3)	116.0(6)	P(1)–Au(1)–Au(4)	125.6(4)	P(6)–Au(6)–Au(2)	126.1(6)	P(6)–Au(6)–Au(5)	125.9(6)
P(1)–Au(1)–Au(5)	134.5(6)	P(1)–Au(1)–Au(6)	120.0(4)	P(6)–Au(6)–Rh	167.7(5)	Au(3)–Au(7)–Au(2)	60.7(1)
P(1)–Au(1)–Rh	172.0(6)	Au(3)–Au(2)–Au(1)	57.5(1)	Rh–Au(7)–Au(2)	57.4(2)	Rh–Au(7)–Au(3)	59.7(2)
Au(6)–Au(2)–Au(1)	53.9(1)	Au(6)–Au(2)–Au(3)	103.5(2)	P(7)–Au(7)–Au(2)	140.6(6)	P(7)–Au(7)–Au(3)	139.0(6)
Au(7)–Au(2)–Au(1)	103.3(1)	Au(7)–Au(2)–Au(3)	58.6(1)	P(7)–Au(7)–Rh	155.0(6)	Au(2)–Rh–Au(1)	69.9(2)
Au(7)–Au(2)–Au(6)	110.4(2)	Rh–Au(2)–Au(1)	55.2(2)	Au(3)–Rh–Au(1)	63.7(2)	Au(3)–Rh–Au(2)	63.9(2)
Rh–Au(2)–Au(3)	59.1(2)	Rh–Au(2)–Au(6)	56.7(2)	Au(4)–Rh–Au(1)	63.3(1)	Au(4)–Rh–Au(2)	120.5(2)
Rh–Au(2)–Au(7)	58.2(2)	P(2)–Au(2)–Au(1)	141.6(5)	Au(4)–Rh–Au(3)	63.6(2)	Au(5)–Rh–Au(1)	71.3(2)
P(2)–Au(2)–Au(3)	137.3(6)	P(2)–Au(2)–Au(6)	117.1(6)	Au(5)–Rh–Au(2)	129.5(3)	Au(5)–Rh–Au(3)	122.4(2)
P(2)–Au(2)–Au(7)	113.8(6)	P(2)–Au(2)–Rh	158.2(4)	Au(5)–Rh–Au(4)	65.0(2)	Au(6)–Rh–Au(1)	61.4(2)
Au(2)–Au(3)–Au(1)	64.9(1)	Au(4)–Au(3)–Au(1)	59.1(1)	Au(6)–Rh–Au(2)	68.1(2)	Au(6)–Rh–Au(3)	115.8(2)
Au(4)–Au(3)–Au(2)	109.2(2)	Au(7)–Au(3)–Au(1)	110.6(2)	Au(6)–Rh–Au(4)	114.0(3)	Au(6)–Rh–Au(5)	65.5(2)
Au(7)–Au(3)–Au(2)	60.7(1)	Au(7)–Au(3)–Au(4)	103.4(1)	Au(7)–Rh–Au(1)	119.8(3)	Au(7)–Rh–Au(2)	64.4(2)
Rh–Au(3)–Au(1)	57.3(2)	Rh–Au(3)–Au(2)	57.0(1)	Au(7)–Rh–Au(3)	62.1(2)	Au(7)–Rh–Au(4)	111.0(3)
Rh–Au(3)–Au(4)	57.7(2)	Rh–Au(3)–Au(7)	58.3(2)	Au(7)–Rh–Au(5)	166.0(2)	Au(7)–Rh–Au(6)	126.2(2)
P(3)–Au(3)–Au(1)	129.3(5)	P(3)–Au(3)–Au(2)	135.7(6)	C(1)–Rh–Au(1)	128.3(22)	C(1)–Rh–Au(2)	89.6(11)
P(3)–Au(3)–Au(4)	113.0(6)	P(3)–Au(3)–Au(7)	119.4(6)	C(1)–Rh–Au(3)	146.5(21)	C(1)–Rh–Au(4)	148.7(15)
P(3)–Au(3)–Rh	166.1(5)	Au(3)–Au(4)–Au(1)	60.3(1)	C(1)–Rh–Au(5)	89.9(24)	C(1)–Rh–Au(6)	67.0(22)
Au(5)–Au(4)–Au(1)	65.8(1)	Au(5)–Au(4)–Au(3)	109.8(1)	C(2)–Rh–Au(1)	128.6(22)	C(2)–Rh–Au(2)	145.7(18)
Rh–Au(4)–Au(1)	58.0(1)	Rh–Au(4)–Au(3)	58.7(2)	C(2)–Rh–Au(3)	96.4(12)	C(2)–Rh–Au(4)	65.5(22)
Rh–Au(4)–Au(5)	55.9(2)	P(4)–Au(4)–Au(1)	149.3(5)	C(2)–Rh–Au(5)	84.5(19)	C(2)–Rh–Au(6)	144.1(13)
P(4)–Au(4)–Au(3)	129.1(6)	P(4)–Au(4)–Au(5)	120.4(6)	C(1)–Rh–Au(7)	88.8(26)	C(2)–Rh–Au(7)	81.7(19)
P(4)–Au(4)–Rh	152.3(5)	Au(4)–Au(5)–Au(1)	56.7(1)	C(2)–Rh–C(1)	95.1(22)	O(1)–C(1)–Rh	159.2(91)
				O(2)–C(2)–Rh	160.7(76)		

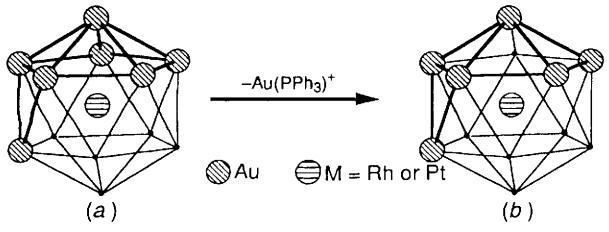

Fig. 6 The structural relationship between $[Rh(CO)_2(AuPPh_3)_7]^{2+}$ **3** (*a*) and $[Pt(PPh_3)(CO)(AuPPh_3)_6]^{2+}$ (*b*)

$(AuPPh_3)_6]^{2+}$,[6] which adopts a metal core geometry that may be derived from the bridged pentagonal-bipyramidal structure of $[Rh(CO)_2(AuPPh_3)_7]^{2+}$ **3** by removal of one $AuPPh_3$ unit from an equatorial position. This relation is shown in Fig. 6. This, and the fact that $[Rh(CO)_2(AuPPh_3)_7]^{2+}$ **3** is formed by addition of $Au(PPh_3)^+$ to $[Rh(CO)_2(AuPPh_3)_6]^+$, suggest that $[Rh(CO)_2(AuPPh_3)_6]^+$ may be isostructural with $[Pt(PPh_3)(CO)(AuPPh_3)_6]^{2+}$.

Conclusion

All rhodium centred gold-cluster compounds introduced in this paper show metal core geometries that are related to a rhodium-centred icosahedron. From a topological point of view the structures of $[Rh(CO)_2(AuPPh_3)_7]^{2+}$ **3**, $[Rh(CO)_2(AuPPh_3)_6]^+$ **4** and $[Rh(CNC_8H_9)_3(AuPPh_3)_5]^{2+}$ **1** may be derived from $[Rh(CNC_8H_9)_2(AuPPh_3)_6(AuCl)_2]^+$ **2** by three sequential removals of $AuPPh_3$ moieties (Fig. 7). Compound **4**, which could not be completely characterised in this study, represents the only member of this series which has not been characterised by single-crystal X-ray diffraction techniques.

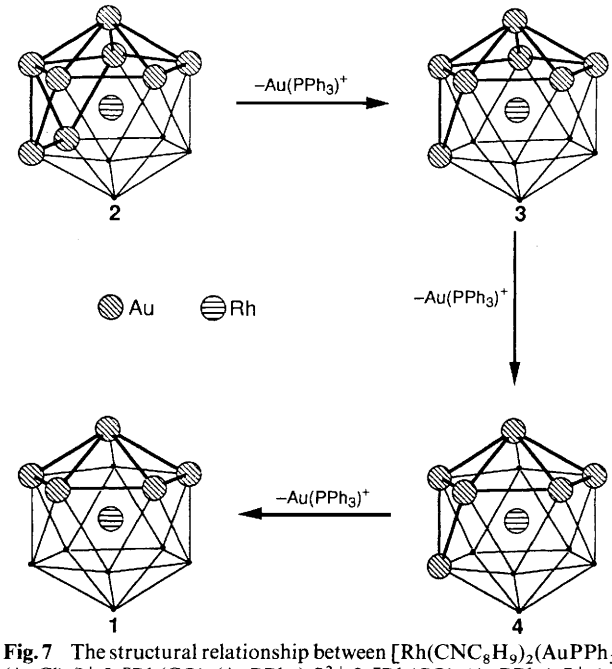

Fig. 7 The structural relationship between $[Rh(CNC_8H_9)_2(AuPPh_3)_6(AuCl)_2]^+$ **3**, $[Rh(CO)_2(AuPPh_3)_7]^{2+}$ **2**, $[Rh(CO)_2(AuPPh_3)_6]^+$ **4** and $[Rh(CNC_8H_9)_3(AuPPh_3)_5]^{2+}$ **1**

Experimental

Reactions were routinely performed using standard Schlenk-line procedures under an atmosphere of pure, dry nitrogen. Solvents were dried, distilled and N_2-saturated prior to use. Elemental analyses (C, H, N and Cl) were carried out by Mr. M. Gascoyne and his staff at this laboratory. Infrared spectra were recorded as Nujol or hexachlorobutadiene (hcbd) mulls on a Perkin-Elmer 1700FT spectrometer. Data in the region 400–250 cm^{-1} were recorded using a Perkin-Elmer 457 spectrometer, calibrated using polystyrene film. Proton and proton-decoupled ^{31}P NMR spectra were routinely recorded in deuteriated

solvents using a Bruker AM-300 spectrometer. Chemical shifts were referenced externally to aqueous solutions of trimethyl phosphate and were taken as positive to high frequency of the reference. Fast atom bombardment mass spectra were run by Dr. J. A. Ballantine and his staff at the SERC Mass Spectrometry Service Centre, University College of Swansea. Experiments were carried out using a VG ZAB-E high-resolution double-focusing mass spectrometer. Samples were suspended in a matrix of *m*-nitrobenzyl alcohol or glycerol and bombarded with a high-energy beam of xenon atoms to generate ions.

Syntheses.—$[Rh(CNC_8H_9)_3(AuPPh_3)_5][PF_6]_2$. A solution of $NaBH_4$ (13.6 mg, 0.36 mmol) in ethanol (10 cm^3) was added dropwise to a suspension of $[Au(PPh_3)Cl]$ (180 mg, 0.36 mmol) and $[Rh(CNC_8H_9)_3Cl]$ (190 mg, 0.36 mmol) in ethanol (10 cm^3). Stirring was continued for 15 min, the resultant red solution concentrated *in vacuo* and filtered to remove unreacted $[Rh(CNC_8H_9)_3Cl]$. Addition of excess of NH_4PF_6 (430 mg, 2.64 mmol) in ethanol (20 cm^3) to the filtrate yielded a red precipitate. This was recrystallised from CH_2Cl_2–Et_2O to give yellow needles of $[Rh(CNC_8H_9)_3(AuPPh_3)_5][PF_6]_2$ (60 mg, 27% based on Au) (Found: C, 44.65; H, 3.30; N, 1.35. $C_{117}H_{102}Au_5F_{12}N_3P_7Rh{\cdot}CH_2Cl_2$ requires C, 44.75; H, 3.30; N, 1.35%). IR (Nujol): ν(CN) at 2118s and 2085s cm^{-1} and ν(PF_6) at 843 cm^{-1}. NMR (CD_2Cl_2): ^1H, δ 1.92 (s, 18 H, CH_3) and 6.77–7.25 (m, 84 H, aromatic protons); ^{31}P-{^1H}, δ 37.1 [d, ^2J(Rh–P) = 8.3] and −150.2 [spt, ^1J(P–F) = 704 Hz]. Yellow-orange crystals suitable for X-ray diffraction of $[Rh(CNC_8H_9)_3(AuPPh_3)_5][ClO_4]_2$, which precipitated after addition of excess of $Mg(ClO_4)_2$ to the initial filtrate, were obtained by dissolving the compound in hot chlorobenzene (80 °C) and cooling to room temperature over a period of 8 h. **CAUTION**: ClO_4^- salts may be explosive.

$[Rh(CNC_8H_9)_2(AuPPh_3)_6(AuCl)_2]PF_6$. The procedure described above for the synthesis of $[Rh(CNC_8H_9)_3(AuPPh_3)_5][PF_6]_2$ was followed. After NH_4PF_6 metathesis to remove $[Rh(CNC_8H_9)_3(AuPPh_3)_5][PF_6]_2$ from the reaction mixture a red filtrate remained. Red crystals of $[Rh(CNC_8H_9)_2(AuPPh_3)_6]PF_6$ suitable for X-ray diffraction were obtained by slow diffusion of hexane into an acetone solution of the filtrate. ^{31}P-{^1H} NMR (CD_2Cl_2): δ 40.9 [d, ^2J(Rh–P) = 9.6] and −150 [spt, ^1J(P–F) = 700 Hz].

$[Rh(CO)_2(AuPPh_3)_7][NO_3]_2$. (*a*) The compound $[Rh(CO)_2(MeCN)_2]NO_3$ was prepared *in situ* by stirring $[Rh(\mu\text{-}Cl)_2(CO)_4]$ (9.7 mg, 2.5×10^{-5} mol) and $AgNO_3$ (9.9 mg, 5.83×10^{-5} mol) in MeCN (10 cm^3) for 30 min. The freshly filtered solution was added to $[Au(PPh_3)(NO_3)]$ (129.5 mg, 2.48×10^{-4} mol) (Au:Rh mol ratio 5:1) and an EtOH solution (10 cm^3) of $NaBH_4$ (9.5 mg, 2.51×10^{-4} mol) was added dropwise. The resultant solution was evaporated to dryness, a red solution extracted with CH_2Cl_2 and the solvent removed *in vacuo*. The residue was washed with Et_2O and toluene and dissolved in thf (10 cm^3). The solution was filtered and the filtrate evaporated to dryness {thf fraction: ^{31}P-{^1H} NMR (CD_2Cl_2) δ 41.03 [d, ^2J(Rh–P) = 11.5 Hz]; IR (Nujol) ν(CO) at 1944m and 1913m cm^{-1} and ν(NO_3) at 1378(sh) cm^{-1}}. The residue was redissolved in thf (10 cm^3) and a solution of $[Au(PPh_3)(NO_3)]$ (25.9 mg, 4.97×10^{-5} mol) added. After cooling to −20 °C, this was filtered and the remaining orange solid recrystallised from CH_2Cl_2–Et_2O to give orange-red crystals of $[Rh(CO)_2(AuPPh_3)_7][NO_3]_2$ (58 mg, 39% based on Au) (Found: C, 43.95; H, 3.05; N, 0.85. $C_{128}H_{105}Au_7N_2O_8P_7Rh$ requires C, 43.95; H, 3.05; N, 0.80%). IR (Nujol): ν(CO) at 1965m and 1943m cm^{-1} and ν(NO_3) at 1377s cm^{-1}. NMR (CD_2Cl_2): ^1H, δ 6.8–7.3 (m, aromatic protons); ^{31}P-{^1H}, δ 41.85 [d, ^2J(Rh–P) = 9.1 Hz]. Single crystals of $[Rh(CO)_2(AuPPh_3)_7][NO_3]_2$ suitable for an X-ray diffraction study were grown by slow diffusion of Et_2O into a CH_2Cl_2 solution of this product.

(*b*) A yellow solution of $[Rh(\mu\text{-}Cl)_2(CO)_4]$ (5.3 mg, 1.36×10^{-5} mol) in CH_2Cl_2 (5 cm^3) was added to a red solution of $[Au_8(PPh_3)_8][NO_3]_2$ (103 mg, 2.71×10^{-5} mol) in CH_2Cl_2 (10 cm^3). The resultant dark red solution was stirred for 30 min and Et_2O added to give $[Au_9(PPh_3)_8][NO_3]_3$ as a green powder. Addition of more Et_2O to the red filtrate yielded orange-red microcrystals of $[Rh(CO)_2(AuPPh_3)_7][NO_3]_2$ (18 mg, 19%).

X-Ray Structure Analysis.—X-Ray diffraction data were collected on an Enraf-Nonius CAD4 diffractometer at room temperature (23 °C) in the Chemical Crystallography Laboratory, University of Oxford. The data were processed on the Chemical Crystallography VAX computer.

Crystal data for complex **1**. $C_{117}H_{103}Au_5Cl_2N_3P_5O_8Rh{\cdot}C_6H_5Cl$, M = 3104.38, triclinic, space group $P\bar{1}$, a = 13.607(4), b = 16.675(6), c = 31.872(9) Å, α = 84.72(3), β = 89.02(3), γ = 81.56(3)°, U = 7122 $Å^3$, $F(000)$ = 2860, μ(Mo-Kα) = 53.66 cm^{-1}, Z = 2, D_c = 1.45 g cm^3.

The crystal selected for data collection had dimensions 0.1 × 0.2 × 1.0 mm and was sealed in a Lindemann capillary tube. An ω–2θ scan with width 0.6 + 0.35tanθ was used to collect data in the range θ 1–15° until the crystal showed a phase transition resulting in a shrinkage of the *c* axis, probably due to loss of solvent. A DIFABS[18] correction varying from 2.57 to 1.56 was applied. 5095 Reflections were collected and equivalent reflections were merged (Sheldrick R_{merg} = 0.025) to give 3489 reflections with $I \geqslant 2.0\,\sigma(I)$.

Structure solution and refinement. The atomic positions of the metal atoms were found from a direct methods (SHELXS)[19] solution. The remaining non-hydrogen atoms were located by subsequent Fourier difference methods using CRYSTALS[20] which was also used for all other calculations. The atomic scattering factors were taken from ref. 21. Blocked-matrix least-squares refinement of 574 parameters converged at final '*R* and *R*' values of 0.0744 and 0.0842. A Chebyschev weighting scheme (parameters 10.2, −3.85, 7.8) was applied. The phenyl rings of the PPh_3 ligands and of the solvent molecule were treated as rigid hexagons (C–C 1.39 Å) and the hydrogen atoms were included in structure-factor calculations at calculated positions (C–H 1.00 Å). The positions of the atoms of the xylyl groups in the isocyanide ligands were refined under restraint of a planar arrangement with C–C distances within the ring of 1.39(3) Å and methyl–carbon to ring–carbon distances of 1.46(2) Å. The ClO_4 anions were refined as idealised tetrahedra with Cl–O distances of 1.46 Å. Anisotropic thermal parameters were assigned to Au, Rh, P, Cl, O, N and to the carbons of the isocyanide ligands during the final cycles of refinement. The relevant positional parameters are given in Table 8.

Crystal data for complex **2**. $C_{126}H_{108}Au_8Cl_2F_6N_2P_7Rh$, M = 3730.63, monoclinic, space group $P2_1/n$, a = 27.748(8), b = 14.546(4), c = 34.04(1) Å, β = 100.12(3)°, U = 13 524 $Å^3$, $F(000)$ = 6992, μ(Mo-Kα) = 89.17 cm^{-1}, Z = 4, D_c = 1.83 g cm^{-3}.

The crystal selected for data collection had dimensions 0.4 × 0.4 × 0.3 mm and was sealed in a Lindemann capillary tube. An ω–2θ scan with width 0.65 + 0.35tanθ was used to collect data in the range θ 1–20°. Azimuthal scan data were used for an absorption correction and the transmission factor varied from 1.30 to 1.00. 13 736 Reflections were collected and equivalent reflections were merged (Sheldrick R_{merg} = 0.055) to give 6508 reflections with $I \geqslant 3.0\,\sigma(I)$.

Structure solution and refinement.[18] The positions of the metal atoms were found from a direct methods (SHELXS) solution. The remaining non-hydrogen atoms were located in subsequent Fourier difference syntheses. Blocked-matrix least-squares refinement of 693 parameters converged at final *R* and *R*' values of 0.0647 and 0.0695. The hydrogen atoms included in structure-factor calculations were generated geometrically. A Chebyschev weighting scheme (parameters 6.003, −1.966, 4.288) was applied. Anisotropic thermal parameters were as-

Table 8 Positional parameters ($\times 10^4$) for compound **1**, with standard deviations in parentheses

Atom	*X/a*	*Y/b*	*Z/c*	Atom	*X/a*	*Y/b*	*Z/c*
Au(1)	2255(1)	664(1)	7515.6(6)	Au(2)	1709(1)	2125(1)	6994.6(6)
Au(3)	2485(1)	1165(1)	8342.1(6)	Au(4)	980(1)	2085(1)	7843.8(6)
Au(5)	1755(1)	3509(1)	7531.3(6)	Rh	2935(2)	2081(2)	7649(1)
P(1)	2344(9)	−695(7)	7411(4)	P(2)	899(9)	2063(7)	6370(4)
P(3)	2510(10)	568(7)	9013(4)	P(4)	−646(9)	2272(7)	8067(4)
P(5)	1263(9)	4899(7)	7426(4)	N(1)	4800(30)	760(20)	7510(10)
N(2)	3990(30)	3060(20)	6960(10)	N(3)	3630(30)	2880(20)	8410(10)
C(1)	4140(30)	1190(20)	7620(10)	C(2)	3550(30)	2680(30)	7200(10)
C(3)	3310(30)	2550(30)	8150(20)	C(11)	5560(30)	250(20)	7410(10)
C(12)	6240(30)	−130(20)	7710(10)	C(13)	6980(20)	−730(20)	7580(10)
C(14)	7030(30)	−950(20)	7180(10)	C(15)	6350(30)	−540(20)	6890(10)
C(16)	5600(20)	70(20)	7000(10)	C(17)	6200(30)	70(20)	8150(10)
C(18)	4870(30)	480(20)	6690(10)	C(21)	4650(20)	3510(20)	6740(10)
C(22)	5250(20)	3990(20)	6930(10)	C(23)	5850(20)	4510(20)	6720(10)
C(24)	5810(20)	4510(20)	6290(10)	C(25)	5250(20)	4080(20)	6060(10)
C(26)	4690(20)	3600(20)	6310(10)	C(27)	5220(30)	3900(20)	7390(10)
C(28)	4060(30)	3110(20)	6110(10)	C(31)	4040(40)	3110(20)	8780(10)
C(32)	5060(40)	3060(20)	8810(20)	C(33)	5360(40)	3470(30)	9140(20)
C(34)	4740(60)	3890(20)	9420(20)	C(35)	3740(50)	3860(20)	9360(10)
C(36)	3340(30)	3480(20)	9050(10)	C(37)	5740(40)	2650(20)	8520(20)
C(38)	2270(30)	3500(20)	9010(10)	C(111)	3140(20)	−1290(20)	7805(8)
C(112)	3910(30)	−980(10)	7990(10)	C(113)	4490(20)	−1440(20)	8300(10)
C(114)	4300(20)	−2220(20)	8433(9)	C(115)	3540(30)	−2540(10)	8250(10)
C(116)	2960(20)	−2080(20)	7940(10)	C(121)	1170(20)	−1110(20)	7450(10)
C(122)	980(20)	−1650(20)	7166(8)	C(123)	150(30)	−2050(20)	7220(10)
C(124)	−490(20)	−1910(20)	7560(10)	C(125)	−300(20)	−1370(20)	7843(9)
C(126)	530(30)	−970(20)	7791(9)	C(131)	2960(30)	−980(20)	6943(8)
C(132)	2440(20)	−670(20)	6580(10)	C(133)	2850(30)	−820(20)	6186(9)
C(134)	3770(30)	−1290(20)	6159(9)	C(135)	4290(20)	−1600(20)	6520(10)
C(136)	3880(20)	−1450(20)	6916(9)	C(211)	1760(20)	1970(20)	5930(10)
C(212)	1680(20)	2490(20)	5560(10)	C(213)	2410(30)	2400(20)	5253(9)
C(214)	3220(20)	1800(20)	5310(10)	C(215)	3310(20)	1280(20)	5680(10)
C(216)	2580(30)	1360(20)	5990(9)	C(221)	320(20)	1140(20)	6380(10)
C(222)	−150(30)	940(20)	6760(9)	C(223)	−680(20)	280(20)	6800(10)
C(224)	−740(20)	−170(20)	6460(10)	C(225)	−270(30)	30(20)	6080(10)
C(226)	260(20)	690(20)	6042(8)	C(231)	−30(20)	2900(20)	6190(10)
C(232)	20(20)	3650(30)	6346(8)	C(233)	−650(30)	4330(20)	6210(10)
C(234)	−1370(20)	4260(20)	5910(10)	C(235)	−1420(20)	3510(30)	5757(8)
C(236)	−750(30)	2830(20)	5900(10)	C(311)	1970(30)	1280(20)	9360(10)
C(312)	1030(30)	1730(30)	9290(10)	C(313)	600(20)	2250(20)	9570(20)
C(314)	1100(40)	2330(20)	9940(10)	C(315)	2040(40)	1890(30)	20(10)
C(316)	2470(20)	1360(20)	9730(20)	C(321)	1810(20)	−310(20)	9100(10)
C(322)	1780(30)	−880(30)	8812(9)	C(323)	1270(30)	−1540(20)	8910(10)
C(324)	800(30)	−1630(20)	9300(20)	C(325)	840(30)	−1060(30)	9590(10)
C(326)	1340(30)	−400(20)	9490(10)	C(331)	3750(20)	200(30)	9190(10)
C(332)	4140(30)	−590(20)	9340(10)	C(333)	5160(30)	−790(20)	9410(10)
C(334)	5780(20)	−200(30)	9330(10)	C(335)	5390(30)	590(20)	9180(10)
C(336)	4370(30)	790(20)	9110(10)	C(411)	−1000(20)	1530(20)	8482(9)
C(412)	−1540(20)	1750(10)	8840(10)	C(413)	−1770(20)	1140(20)	9140(8)
C(414)	−1470(30)	330(20)	9080(10)	C(415)	−940(30)	110(10)	8720(10)
C(416)	−700(20)	720(20)	8424(9)	C(421)	−1560(20)	2290(20)	7662(9)
C(422)	−2310(30)	1810(20)	7681(9)	C(423)	−2940(20)	1840(20)	7340(10)
C(424)	−2820(20)	2350(20)	6980(10)	C(425)	−2060(30)	2830(20)	6960(9)
C(426)	−1440(20)	2810(20)	7300(10)	C(431)	−970(30)	3250(10)	8286(9)
C(432)	−1920(20)	3690(20)	8256(9)	C(433)	−2120(20)	4450(20)	8410(10)
C(434)	−1370(30)	4770(10)	8600(10)	C(435)	−410(30)	4330(20)	8630(10)
C(436)	−210(20)	3570(20)	8470(10)	C(511)	2070(20)	5370(20)	7055(9)
C(512)	2320(20)	6130(20)	7120(8)	C(513)	2910(20)	6520(10)	6830(10)
C(514)	3250(20)	6140(20)	6470(10)	C(515)	3000(20)	5380(20)	6406(8)
C(516)	2410(20)	5000(10)	6700(10)	C(521)	1330(30)	5380(20)	7902(8)
C(522)	2170(20)	5160(20)	8150(10)	C(523)	2260(20)	5530(20)	8520(10)
C(524)	1510(30)	6120(20)	8638(8)	C(525)	670(20)	6350(20)	8390(10)
C(526)	580(20)	5980(20)	8020(10)	C(531)	40(20)	5240(20)	7230(10)
C(532)	−740(30)	4860(10)	7400(8)	C(533)	−1700(20)	5120(20)	7260(10)
C(534)	−1890(20)	5760(20)	6940(10)	C(535)	−1110(30)	6130(20)	6768(8)
C(536)	−140(20)	5870(20)	6910(10)				

signed to Au, Rh, P and Cl during the final cycles of refinement. The relevant positional parameters are given in Table 9.

Crystal data for complex **3**. $C_{128}H_{105}Au_7N_2O_8P_7Rh$, M = 3497.74, monoclinic, space group $P2_1/c$, a = 18.051(6), b = 38.836(10), c = 19.860(5) Å, β = 114.6(3)°, U = 12 654 Å^3, $F(000)$ = 6616, μ(Mo-Kα) = 83.34 cm^{-1}, Z = 4, D_c = 1.84 g cm^{-3}.

The crystal selected for data collection had dimensions 0.16 × 0.2 × 0.16 mm and was mounted on a glass fibre. An ω–2θ scan with width 0.6 + 0.35tanθ was used to collect data in

Table 9 Positional parameters ($\times 10^4$) for compound **2**, with standard deviations in parentheses

Atom	*X*/*a*	*Y*/*b*	*Z*/*c*	Atom	*X*/*a*	*Y*/*b*	*Z*/*c*
Au(1)	4 804.7(5)	6 603.7(9)	1 933.4(4)	Au(2)	5 260.5(5)	4 885.6(9)	1 919.1(4)
Au(3)	5 606.2(5)	5 078(1)	3 359.4(4)	Au(4)	5 024.0(5)	6 665.2(9)	3 314.8(4)
Au(5)	4 313.0(5)	6 570.3(9)	2 608.6(4)	Au(6)	5 150.9(5)	3 955.8(9)	2 656.7(4)
Au(7)	4 558.2(5)	4 950.6(9)	3 083.9(4)	Au(8)	4 362.0(5)	4 942.0(9)	2 183.8(4)
Rh	5 201(1)	5 781(2)	2 631.8(8)	P(1)	4 687(4)	7 646(7)	1 428(3)
P(2)	5 577(4)	4 149(6)	1 429(3)	P(3)	6 191(3)	4 599(6)	3 882(3)
P(4)	4 961(4)	7 729(7)	3 798(3)	P(7)	4 023(4)	4 186(6)	3 405(3)
P(8)	3 690(4)	4 264(6)	1 798(3)	Cl(1)	3 577(4)	7 383(6)	2 577(3)
Cl(2)	5 240(5)	2 373(6)	2 684(4)	N(1)	6 248(10)	5 254(19)	2 589(8)
N(2)	5 615(11)	7 749(19)	2 700(9)	C(1)	4 747(14)	7 161(27)	935(12)
C(2)	4 940(18)	7 711(31)	667(15)	C(3)	4 937(21)	7 216(40)	292(17)
C(4)	4 762(17)	6 424(33)	219(14)	C(5)	4 605(18)	5 915(33)	491(15)
C(6)	4 553(17)	6 305(31)	835(14)	C(7)	5 155(14)	8 521(26)	1 507(11)
C(8)	5 655(14)	8 239(25)	1 659(11)	C(9)	6 011(20)	8 927(38)	1 731(16)
C(10)	5 945(18)	9 839(34)	1 671(14)	C(11)	5 483(22)	10 067(41)	1 546(17)
C(12)	5 077(16)	9 457(29)	1 432(13)	C(13)	4 098(16)	8 272(30)	1 347(13)
C(14)	3 904(15)	8 708(26)	999(12)	C(15)	3 440(18)	9 135(31)	961(15)
C(16)	3 228(17)	9 164(30)	1 277(14)	C(17)	3 407(17)	8 808(30)	1 652(14)
C(18)	3 835(14)	8 272(27)	1 655(12)	C(19)	6 107(13)	3 437(24)	1 661(10)
C(20)	6 548(19)	3 606(34)	1 579(15)	C(21)	6 940(17)	3 014(33)	1 758(14)
C(22)	6 833(23)	2 328(41)	1 980(18)	C(23)	6 410(18)	2 164(30)	2 041(14)
C(24)	6 021(14)	2 778(25)	1 879(11)	C(25)	5 166(13)	3 348(25)	1 131(10)
C(26)	5 328(16)	2 557(27)	971(12)	C(27)	4 975(21)	2 018(37)	754(17)
C(28)	4 499(23)	2 190(41)	635(18)	C(29)	4 328(18)	3 012(33)	728(14)
C(30)	4 687(17)	3 616(30)	1 003(13)	C(31)	5 811(16)	4 870(30)	1 089(13)
C(32)	5 933(17)	4 563(30)	722(14)	C(33)	6 126(18)	5 132(35)	481(15)
C(34)	6 193(19)	6 101(35)	551(16)	C(35)	6 060(20)	6 465(38)	919(16)
C(36)	5 864(18)	5 789(33)	1 160(15)	C(37)	6 829(14)	4 818(27)	3 805(11)
C(38)	6 877(19)	5 640(35)	3 627(15)	C(39)	7 333(19)	5 859(33)	3 552(15)
C(40)	7 706(15)	5 296(29)	5 653(12)	C(41)	7 652(17)	4 523(32)	3 840(14)
C(42)	7 200(16)	4 229(28)	3 928(13)	C(43)	6 174(12)	5 180(23)	4 339(10)
C(44)	5 725(14)	5 502(26)	4 415(12)	C(45)	5 683(16)	5 970(31)	4 761(14)
C(46)	6 133(21)	6 103(37)	5 039(16)	C(47)	6 584(19)	5 809(34)	4 959(16)
C(48)	6 602(16)	5 333(30)	4 619(13)	C(49)	6 178(13)	3 387(25)	3 993(10)
C(50)	6 414(13)	3 018(22)	4 360(10)	C(51)	6 393(14)	2 090(25)	4 447(11)
C(52)	6 120(17)	1 566(33)	4 145(14)	C(53)	5 879(17)	1 871(32)	3 767(14)
C(54)	5 897(16)	2 815(30)	3 729(13)	C(55)	4 721(14)	8 844(25)	3 605(10)
C(56)	4 944(17)	9 664(30)	3 574(13)	C(57)	4 666(25)	10 435(46)	3 503(21)
C(58)	4 224(22)	10 400(39)	3 243(17)	C(59)	3 999(17)	9 586(32)	3 239(14)
C(60)	4 233(15)	8 746(27)	3 359(12)	C(61)	4 578(16)	7 382(29)	4 133(13)
C(62)	4 343(18)	7 985(32)	4 355(15)	C(63)	4 053(24)	7 648(44)	4 624(19)
C(64)	4 033(19)	6 705(38)	4 682(16)	C(65)	4 217(16)	6 195(30)	4 472(13)
C(66)	4 501(17)	6 459(31)	4 187(14)	C(67)	5 546(14)	8 033(25)	4 097(11)
C(68)	5 587(20)	8 418(38)	4 481(16)	C(69)	6 033(27)	8 700(46)	4 693(20)
C(70)	6 426(21)	8 493(39)	4 526(17)	C(71)	6 440(25)	8 000(46)	4 187(22)
C(72)	5 932(23)	7 856(39)	3 972(18)	C(73)	3 599(12)	4 910(23)	3 596(9)
C(74)	3 317(13)	4 710(24)	3 908(11)	C(75)	3 034(14)	5 328(26)	4 013(11)
C(76)	2 930(15)	6 162(28)	3 857(13)	C(77)	3 165(17)	6 419(31)	3 568(14)
C(78)	3 504(18)	5 792(33)	3 442(15)	C(79)	4 330(14)	3 471(27)	3 818(11)
C(80)	4 735(17)	3 837(30)	4 047(14)	C(81)	4 995(16)	3 338(32)	4 356(13)
C(82)	4 805(16)	2 482(28)	4 470(13)	C(83)	4 408(19)	2 155(34)	4 266(16)
C(84)	4 102(16)	2 662(29)	3 920(13)	C(85)	3 657(14)	3 322(26)	3 087(11)
C(86)	3 880(14)	2 797(26)	2 842(12)	C(87)	3 640(17)	2 118(29)	2 588(13)
C(88)	3 172(20)	2 014(36)	2 640(16)	C(89)	2 918(18)	2 479(32)	2 883(15)
C(90)	3 182(16)	3 164(28)	3 102(12)	C(91)	3 153(13)	4 296(24)	2 031(11)
C(92)	3 132(16)	4 934(33)	2 316(13)	C(93)	2 708(23)	5 049(43)	2 535(18)
C(94)	2 324(18)	4 532(33)	2 412(15)	C(95)	2 337(17)	3 940(31)	2 111(14)
C(96)	2 721(17)	3 741(29)	1 963(13)	C(97)	3 470(13)	4 904(26)	1 328(11)
C(98)	3 432(23)	4 466(42)	956(19)	C(99)	3 262(19)	5 109(40)	631(16)
C(100)	3 211(21)	6 006(41)	679(18)	C(101)	3 294(19)	6 340(35)	1 054(17)
C(102)	3 425(16)	5 817(29)	1 383(13)	C(103)	3 764(15)	3 087(27)	1 672(12)
C(104)	4 204(17)	2 791(31)	1 842(14)	C(105)	4 311(18)	1 712(34)	1 756(14)
C(106)	3 977(18)	1 235(31)	1 558(14)	C(107)	3 566(16)	1 586(30)	1 393(11)
C(108)	3 427(14)	2 559(24)	1 450(11)	C(109)	5 801(14)	5 328(25)	2 595(11)
C(110)	6 732(14)	4 921(27)	2 556(11)	C(111)	6 995(13)	5 551(24)	2 368(11)
C(112)	7 521(16)	5 266(29)	2 394(13)	C(113)	7 650(18)	4 444(34)	2 582(15)
C(114)	7 419(19)	3 619(34)	2 775(15)	C(115)	6 888(13)	4 111(23)	2 751(10)
C(116)	6 840(18)	6 427(34)	2 171(15)	C(117)	6 589(15)	3 512(28)	2 934(12)
C(118)	5 372(12)	6 992(21)	2 663(9)	C(119)	5 818(12)	8 615(21)	2 822(9)
C(120)	5 460(15)	9 339(27)	2 701(12)	C(121)	5 627(18)	10 139(34)	2 787(14)
C(122)	6 052(19)	10 346(32)	2 950(14)	C(123)	6 412(15)	9 656(28)	3 069(12)
C(124)	6 305(17)	8 681(31)	3 028(14)	C(125)	4 970(22)	9 219(38)	2 544(17)
C(126)	6 575(19)	7 837(35)	3 075(16)				

Table 10 Positional parameters ($\times 10^4$) for compound **3**, with standard deviations in parentheses

Atom	*X/a*	*Y/b*	*Z/c*	Atom	*X/a*	*Y/b*	*Z/c*
Au(1)	4046(3)	3885.4(7)	2928(2)	Au(2)	2325(3)	3999.3(8)	1669(2)
Au(3)	2611(3)	3549.6(8)	2915(2)	Au(4)	4106(3)	3167.9(7)	3262(2)
Au(5)	4783(3)	3343.1(8)	2222(2)	Au(6)	3922(3)	3966.4(8)	1490(2)
Au(7)	1588(3)	3324.2(8)	1468(2)	Rh	3213(5)	3417(1)	1869(3)
P(1)	4584(13)	4323(4)	3785(8)	P(2)	1426(15)	4429(4)	1043(9)
P(3)	2151(15)	3518(5)	3842(10)	P(4)	4654(15)	2723(4)	4094(9)
P(5)	6060(17)	3208(5)	2261(10)	P(6)	4389(14)	4370(14)	929(9)
P(7)	364(16)	3060(5)	866(11)	O(1)	2689(37)	3390(11)	256(24)
O(2)	3040(35)	2663(11)	1827(24)	C(1)	2997(50)	3422(11)	817(25)
C(2)	3214(43)	2920(12)	1948(37)	C(111)	5040(21)	4677(7)	3517(21)
C(112)	4741(26)	5009(7)	3495(23)	C(113)	5113(32)	5285(7)	3314(24)
C(114)	5784(32)	5230(10)	3155(23)	C(115)	6083(27)	4898(12)	3177(24)
C(116)	5711(22)	4622(9)	3358(22)	C(121)	3755(20)	4504(9)	3942(12)
C(122)	3057(20)	4614(11)	3345(15)	C(123)	2448(22)	4786(11)	3467(23)
C(124)	2538(26)	4847(11)	4186(26)	C(125)	3236(28)	4737(11)	4784(21)
C(126)	3844(24)	4565(11)	4662(14)	C(131)	5351(23)	4184(6)	4685(17)
C(132)	5835(26)	4427(8)	5193(18)	C(133)	6452(27)	4321(11)	5860(19)
C(134)	6584(28)	3972(12)	6019(20)	C(135)	6100(32)	3729(9)	5512(22)
C(136)	5484(28)	3835(6)	4845(21)	C(211)	1392(26)	4467(6)	122(17)
C(212)	1258(34)	4748(7)	−224(20)	C(213)	1156(36)	4812(11)	−956(20)
C(214)	1188(34)	4517(13)	−1342(18)	C(215)	1322(38)	4197(11)	−996(20)
C(216)	1424(33)	4172(8)	−264(20)	C(221)	1570(18)	4870(8)	1417(20)
C(222)	2325(21)	5030(10)	1645(23)	C(223)	2440(31)	5359(10)	1948(23)
C(224)	1800(37)	5528(8)	2023(23)	C(225)	1045(33)	5368(9)	1795(25)
C(226)	930(23)	5039(9)	1492(23)	C(231)	382(23)	4315(10)	886(12)
C(232)	−241(24)	4333(11)	177(14)	C(233)	−1037(23)	4257(11)	61(21)
C(234)	−1211(25)	4163(11)	655(26)	C(235)	−589(28)	4145(11)	1365(23)
C(236)	208(26)	4221(11)	1480(16)	C(311)	1215(23)	3771(7)	3623(21)
C(312)	1217(28)	4123(7)	3505(22)	C(313)	537(33)	4320(9)	3408(24)
C(314)	−147(29)	4164(12)	3429(23)	C(315)	−150(24)	3811(12)	3546(24)
C(232)	−241(24)	4333(11)	177(14)	C(233)	−1037(23)	4257(11)	61(21)
C(234)	−1211(25)	4163(11)	655(26)	C(235)	−589(28)	4145(11)	1365(23)
C(236)	208(26)	4221(11)	1480(16)	C(311)	1215(23)	3771(7)	3623(21)
C(312)	1217(28)	4123(7)	3505(22)	C(313)	537(33)	4320(9)	2408(24)
C(314)	−147(29)	4164(12)	3429(23)	C(315)	−150(24)	3811(12)	3546(24)
C(334)	1622(34)	2363(8)	4007(27)	C(335)	1262(34)	2533(9)	3329(23)
C(336)	1390(28)	2883(9)	3286(17)	C(411)	4475(26)	2711(6)	4926(18)
C(412)	4643(31)	3000(8)	5380(21)	C(413)	4577(35)	2982(11)	6053(20)
C(414)	4343(35)	2676(12)	6270(20)	C(415)	4174(36)	2388(11)	5816(23)
C(416)	4240(31)	2405(8)	5144(21)	C(421)	5741(24)	2677(6)	4428(20)
C(422)	6210(25)	2955(8)	4393(22)	C(423)	7054(25)	2926(11)	4689(25)
C(424)	7429(24)	2620(12)	5021(24)	C(425)	6960(26)	2342(10)	5056(24)
C(426)	6116(26)	2371(7)	4759(22)	C(431)	4146(19)	2334(8)	3598(18)
C(432)	4551(26)	2114(9)	3312(22)	C(433)	4132(35)	1846(9)	2844(23)
C(434)	3308(35)	1798(9)	2662(21)	C(435)	2902(26)	2017(11)	2948(24)
C(436)	3322(19)	2285(10)	3417(22)	C(511)	6330(28)	2760(8)	2312(17)
C(512)	6288(32)	2554(9)	2867(20)	C(513)	6476(34)	2205(9)	2895(25)
C(514)	6706(34)	2063(8)	2367(27)	C(515)	6748(34)	2270(10)	1812(25)
C(516)	6560(31)	2618(9)	1785(20)	C(521)	6866(21)	3407(8)	3060(18)
C(522)	6681(27)	3672(9)	3436(21)	C(523)	7293(33)	3817(10)	4061(21)
C(524)	8089(31)	3697(12)	4310(20)	C(525)	8273(23)	3432(12)	3934(23)
C(526)	7662(20)	3287(10)	3309(21)	C(531)	6176(18)	3375(10)	1447(15)
C(532)	6947(21)	3455(11)	1493(20)	C(533)	7040(30)	3565(12)	865(24)
C(534)	6361(36)	3595(11)	192(21)	C(535)	5590(32)	3515(11)	146(24)
C(536)	5497(22)	3405(11)	733(16)	C(611)	5477(22)	4454(6)	1354(18)
C(612)	6006(23)	4213(8)	1833(20)	C(613)	6835(23)	4284(11)	2188(22)
C(614)	7136(23)	4596(13)	2063(24)	C(615)	6607(25)	4836(10)	1584(25)
C(616)	5778(24)	4765(7)	1229(21)	C(621)	3921(24)	4797(8)	818(12)
C(622)	3436(30)	4921(10)	114(14)	C(623)	3149(34)	5258(10)	23(21)
C(624)	3347(34)	5471(9)	636(25)	C(625)	3831(34)	5348(9)	1341(23)
C(626)	4118(30)	5011(9)	1432(15)	C(631)	4184(19)	4222(9)	8(17)
C(632)	4706(24)	4314(11)	−316(20)	C(633)	4507(33)	4231(12)	−1053(20)
C(634)	3786(35)	4057(11)	−1465(17)	C(635)	3265(29)	3965(12)	−1140(20)
C(636)	3464(22)	4048(10)	−404(20)	C(711)	−233(25)	2977(6)	1387(20)
C(712)	−371(28)	3239(8)	1798(22)	C(713)	−814(30)	3172(11)	2212(23)
C(714)	−1119(29)	2844(12)	2216(24)	C(715)	−981(29)	2582(10)	1805(25)
C(716)	−538(27)	2648(7)	1390(23)	C(721)	−359(20)	3257(9)	11(18)
C(722)	−1190(19)	3241(10)	−169(21)	C(723)	−1740(24)	3405(12)	−803(22)
C(724)	−1460(32)	3585(11)	−1256(19)	C(725)	−629(34)	3600(11)	−1075(19)
C(726)	−79(27)	3436(10)	−442(20)	C(731)	572(21)	2633(8)	589(13)
C(732)	95(29)	2511(10)	−119(15)	C(733)	157(33)	2169(10)	−295(22)
C(734)	696(34)	1949(8)	238(26)	C(735)	1173(33)	2071(9)	946(24)
C(736)	1111(26)	2413(9)	1121(18)				

the range θ 1–7.5° before the crystal decomposed. A DIFABS correction varying from 1.92 to 1.00 was applied. 4673 Reflections were collected and equivalent reflections were merged (Sheldrick R_{merg} = 0.0685) to give 1906 reflections with $I \geqslant 3.0\ \sigma(I)$.

Structure solution and refinement.[18] The positions of the metal atoms were found from a direct methods (SHELXS) solution. The positions of the remaining non-hydrogen atoms with the exception of the phenyl carbons were located in subsequent Fourier difference syntheses. The phenyl rings of the PPh_3 ligands were modelled as rigid groups in idealised positions and the carbon atoms were refined with equivalent thermal parameters. Full-matrix least-squares refinement of 244 parameters converged at final R and R' values of 0.0641 and 0.0722. The hydrogen atoms included in the structure-factor calculations were generated geometrically. A Chebyschev weighting scheme (parameters 4.21, −0.34, 3.17) was applied. Anisotropic thermal parameters were assigned to Au and Rh during the final cycles of refinement. The relevant positional parameters are given in Table 10.

Additional material available from the Cambridge Crystallographic Data Centre comprises H-atom coordinates, thermal parameters and remaining bond lengths and angles.

References

1 K. P. Hall and D. M. P. Mingos, *Prog. Inorg. Chem.*, 1984, **32**, 237; D. M. P. Mingos, *Gold Bull.*, 1984, **17**, 5.

2 F. Scherbaum, A. Grohmann, B. Huber, C. Krüger and H. Schmidbaur, *Angew. Chem., Int. Ed. Engl.*, 1988, **27**, 1544; F. Scherbaum, A. Grohmann, G. Müller and H. Schmidbaur, *Angew. Chem., Int. Ed. Engl.*, 1989, **28**, 463; A. Grohmann, J. Riede and H. Schmidbauer, *Nature (London)*, 1990, **345**, 140; O. Steigelmann, P. Bissinger and H. Schmidbaur, *Angew. Chem., Int. Ed. Engl.*, 1990, **29**, 1399.

3 J. J. Bour, R. P. F. Kanters, P. P. J. Schlebos and J. J. Steggerda, *Recl. Trav. Chim. Pays-Bas*, 1988, **107**, 211; J. J. Bour, R. P. F. Kanters, P. P. J. Schlebos, W. P. Bosman, H. Behm, P. T. Beurskens and J. J. Steggerda, *Recl. Trav. Chim. Pays-Bas*, 1987, **106**, 157.

4 K. P. Hall, B. R. C. Theobald, D. I. Gilmour, D. M. P. Mingos and A. J. Welch, *J. Chem. Soc., Chem. Commun.*, 1982, 528.

5 L. N. Ito, A. M. P. Felicissimo and L. H. Pignolet, unpublished work.

6 L. N. Ito, J. D. Sweet, A. M. Mueting, L. P. Pignolet, M. F. J. Schoondergang and J. J. Steggerda, *Inorg. Chem.*, 1989, **28**, 3696.

7 G. Beuter and J. Strähle, *Angew. Chem., Int. Ed. Engl.*, 1988, **27**, 1094.

8 S. G. Bott, D. M. P. Mingos and M. J. Watson, *J. Chem. Soc., Chem. Commun.*, 1989, 1192.

9 N. J. Claydon, C. M. Dobson, K. P. Hall, D. M. P. Mingos and D. J. Smith, *J. Chem. Soc., Dalton Trans.*, 1985, 1811.

10 P. D. Boyle, B. J. Johnson, A. Buehler and L. H. Pignolet, *Inorg. Chem.*, 1986, **25**, 5.

11 D. M. P. Mingos, *J. Chem. Soc., Dalton Trans.*, 1976, 1163.

12 D. M. P. Mingos and Z. Lin, *Comments Inorg. Chem.*, 1989, **9**, 95.

13 C. E. Briant, B. R. C. Theobald, J. W. White, L. K. Bell and D. M. P. Mingos, *J. Chem. Soc., Chem. Commun.*, 1981, 201; C. E. Briant, K. P. Hall, A. C. Wheeler and D. M. P. Mingos, *J. Chem. Soc., Chem., Commun.*, 1984, 248.

14 R. P. F. Kanters, P. P. J. Schlebos, J. J. Bour, W. P. Bosman, H. J. Behm and J. J. Steggerda, *Inorg. Chem.*, 1988, **27**, 4034.

15 J. G. M. van der Linden, A. M. Roelofson and G. H. W. Ipskamp, *Inorg. Chem.*, 1989, **28**, 967.

16 L. N. Ito, A. M. P. Felicissimo and L. H. Pignolet, unpublished work.

17 M. Manassero, L. Naldini and M. Sansoni, *J. Chem. Soc., Chem. Commun.*, 1979, 385; F. A. Vollenbroek, W. P. Bosman, J. J. Bour, J. H. Noordik and P. T. Beurskens, *J. Chem. Soc., Chem. Commun.*, 1979, 387.

18 N. Walker and D. Stuart, *Acta Crystallogr., Sect. A*, 1983, **39**, 158.

19 G. M. Sheldrick, *Crystallographic Computing 3*, eds. G. M. Sheldrick, C. Kruger and R. Goddard, Oxford University Press, Oxford, 1985, p. 179.

20 D. J. Watkins, J. R. Carruthers and B. W. Bethridge, *CRYSTALS user guide*, Chemical Crystallography Laboratory, Oxford, 1985.

21 *International Tables for X-Ray Crystallography*, Kynoch Press, Birmingham, 1974, vol. 4.

Received 25*th March* 1991; *Paper* 1/01409I